The Boundary Shift Integral: An Accurate and Robust Measure of Cerebral Volume Changes from Registered Repeat MRI

Peter A. Freeborough* and Nick C. Fox

***Abstract*— We propose the *boundary shift integral* (BSI) as a measure of cerebral volume changes derived from registered repeat three-dimensional (3-D) magnetic resonance (MR) [3D MR] scans. The BSI determines the total volume through which the boundaries of a given cerebral structure have moved and, hence, the volume change, directly from voxel intensities. We found brain and ventricular BSI's correlated tightly ($r = 1.000$ and $r = 0.999$) with simulated volumes of change. Applied to 21 control scan pairs and 11 scan pairs from Alzheimer's disease (AD) patients (mean interval 386 days) the BSI yielded mean brain volume loss of 1.8 cc (controls) and 34.7 cc (AD); the control group was tightly bunched (SD = 3.8 cc) and there was wide group separation, the group means differing by 8.7 control group satndard deviations (SD's). A measure based on the same segmentation used by the BSI yielded similar group means, but wide spread in the control group (SD = 13.4 cc) and group overlap, the group means differing by 2.8 control group SD's. The BSI yielded mean ventricular volume losses of 0.4 cc (controls) and 10.1 cc (AD). Good linear correlation ($r = 0.997$) was obtained between the ventricular BSI and the difference in their segmented volumes. We conclude the BSI is an accurate and robust measure of regional and global cerebral volume changes.**

***Index Terms*—Atrophy, brain, MRI, registration.**

I. Introduction

IN THE EARLY stages of a neurodegenerative disease, the accumulated tissue loss is unlikely to yield structural volumes outside the wide natural range and, hence, a direct measure of *change* is likely to be a better diagnostic marker; such early diagnosis may become critical in disorders, such as Alzheimer's disease (AD), for which disease inhibiting drugs are in development. Further, in assessing potential drug treatments, accurate measures of volume change may also provide an objective measure of efficacy.

We have previously shown a global measure of volume change may be obtained by registration of repeat three-dimensional (3-D) magnetic resonance (MR) [3D MR] scans of the same subject, followed by integration of the difference in voxel intensities over only those brain voxels which differ by more than a threshold figure [1]. Although a useful diagnostic marker, the approach implicitly assumes simplistic models for tissue loss and image formation and, hence, does not yield a measure of the *actual* loss in volume. Furthermore, exclusion of intensity differences below the threshold level means the more subtle changes are not accounted for—these may be the very changes of interest.

In this paper, we develop, apply and evaluate a new approach to quantifying volume change between registered repeat scans. We demonstrate its application to measuring both global and regional volume changes.

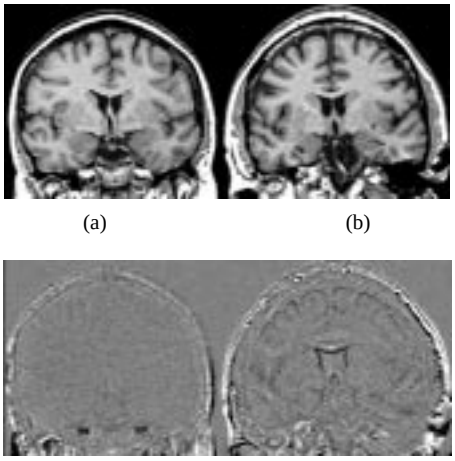

(a) (b)

(c) (d)

Fig. 1. Coronal slices through T1-weighted 3D MR scans of (a) a normal control and (b) an AD patient. Repeat scans were acquired over one year later and registered to these baselines. Difference between baseline and registered repeat scans are shown in (c) and (d), respectively.

II. Nature and Imaging of Cererbral Volume Changes

A. Visualization of Volume Changes

Accurate registration of serial 3D MR scans permits the visualization of subtle changes within the brain [2]–[5]. Fig. 1(a) and 1(b) shows baseline scans of a normal control and an AD patient, respectively. Fig. 1(c) shows the difference between the baseline scan of the normal control and a registered repeat scan acquired over one year later; the difference is represented using a linear intensity scale where white represents an in-

Manuscript received November 7, 1996. The work of P. A. Freeborough was supported by a grant from the Charles Wolfson Charitable Trust. The work of N. C. Fox was done under an Alzheimer's Disease Society (U.K.) Fellowship. The Associate Editor responsible for coordinating the review of this paper and recommending its publication was M. W. Vannier. *Asterisk indicates corresponding author*.

*P. A. Freeborough is with the Dementia Research Group, National Hospital for Neurology and Neurosurgery, 8–11 Queen Square, London WC1N 3BG U.K. (e-mail: paf@ic.ac.uk).

N. C. Fox is with the Dementia Research Group, National Hospital for Neurology and Neurosurgery, London WC1N 3BG U.K.

Publisher Item Identifier S 0278-0062(97)07786-0.

crease, mid-gray no change, and black a decrease in intensity. Note, there is near complete cancellation of intensities within the brain, indicating little or no change over the interval. Correspondingly, Fig. 1(d) compares the baseline scan of the AD patient to a repeat scan acquired after a similar interval; note, there is significant loss of intensity (representing volume loss), particularly around the ventricular system, but also around the cortical surface. Using this methodology patterns of loss have been observed in AD patients using scan intervals as short as three months [2].

B. Boundary Shifts

Histopathological studies of the brain in AD show that the hallmarks of the disease are amyloid plaques, neurofibrillary tangles, and cell death. These changes are distributed widely and diffusely throughout the brain, and while some areas are more affected than others, there is not a greater tendency for cell death to take place at the cortical or ventricular surfaces. The points of intensity loss seen in Fig. 1(d) are, therefore, unlikely to represent the actual location of cell death. They are, most likely, a consequence of structural readjustment to changes elsewhere in the brain, resulting in the shifting of tissue near the boundaries which we observe as a loss of intensity on the difference image.

We assume that differences between registered scans near the boundaries of cerebral structures are associated solely with the shifting of adjacent tissue; any local tissue loss or "gain" being negligible compared to the effects of a global volume change. Where this assumption does not hold, tissue loss or "gain" near the boundary may, to a first approximation, be modeled as a local shift.

C. Image Intensity Formation

The acquisition of true 3D MR scans can be modeled as the digitization of a nonbandlimited continuous signal (i.e., the MR point response of brain tissue) in a two-stage process consisting of ideal lowpass filtering followed by multiplication with a perfect comb function (i.e., ideal sampling at above the Nyquist rate). As multiplication by a comb function in the time domain is equivalent to convolution with a comb function in the frequency domain, the power spectrum of the final signal consists of that of the intermediate lowpass filtered signal plus nonoverlapping high frequency duplicates. Perfect reconstruction of the intermediate lowpass filtered signal from the samples is possible, and is achieved by removing the high frequency duplicates by convoluting the samples with a sinc function (i.e., ideal lowpass filtering); we will refer to these *continuous* intermediate signals as $i_{\mathrm{base}}(x,y,z)$ and $i_{\mathrm{repeat}}(x,y,z)$ on the baseline and repeat scans respectively.

If we construct a continuous function $i_{\mathrm{reg}}(x,y,z)$ by a rigid body transformation of the coordinate system of $i_{\mathrm{repeat}}(x,y,z)$ to match that of $i_{\mathrm{base}}(x,y,z)$—so compensating for different positioning of the head in the scanner—then it follows that if there has been no change in the brain during the interval between the scans, $i_{\mathrm{reg}}(x,y,z)$ and $i_{\mathrm{base}}(x,y,z)$ should be exactly equivalent; as should any discrete samplings of these signals. Furthermore, where the tissue near the boundary of a cerebral structure has shifted, then, in the area around the boundary $i_{\mathrm{reg}}(x,y,z)$ and $i_{\mathrm{base}}(x,y,z)$ should differ only by the exact same positional shift (the associated phase shift being unaffected by the low-pass filter); this permits the precise measurement of such boundary shifts.

III. Measurement

A. Registration

The repeat scan is registered to the baseline by determining the rotations and translations required to minimize the standard deviation of the ratio between corresponding voxels within the brain, while in parallel, determining spatial scaling factors so as to minimize the mean square distance between corresponding voxels on the surface of the cranium. The method incorporates scaling factors based on the cranial surface so as to correct for changes in voxel size which may mimic cerebral volume changes [6]. Sinc interpolation is used for re-sampling. The procedure has been shown to achieve registration accurate to a fraction of a voxel [2].

B. Internal and Boundary Regions

We define the set of voxels corresponding to a given structure on the baseline and registered repeat scans using interactive morphology based procedures followed by manual editing where necessary [7], [8]; we refer to these sets as $\boldsymbol{S}_{\mathbf{base}}$ and $\boldsymbol{S}_{\mathbf{reg}}$ respectively. We also utilize the morphological operator $\boldsymbol{B}$, consisting of the origin and its six immediate neighbors in three dimensions. We define the internal region, $\boldsymbol{T}$, as the intersection of $\boldsymbol{S}_{\mathbf{base}}$ and $\boldsymbol{S}_{\mathbf{reg}}$ eroded by an operator of size N_e, such that

$$\boldsymbol{T} = (\boldsymbol{S}_{\mathbf{base}} \cap \boldsymbol{S}_{\mathbf{reg}}) \oplus (\boldsymbol{B} \oplus \boldsymbol{B} \oplus \cdot \oplus \boldsymbol{B}) \tag{1}$$

where $\boldsymbol{B}$ occurs N_e times on the right hand side.

Similarly, we define a boundary region, $\boldsymbol{E}$, as the set of voxels which are members of the union of $\boldsymbol{S}_{\mathbf{base}}$ and $\boldsymbol{S}_{\mathbf{reg}}$ dilated by an operator of size N_d, while also not being members of the interior set $\boldsymbol{T}$, that is

$$\boldsymbol{E} = ((\boldsymbol{S}_{\mathbf{base}} \cup \boldsymbol{S}_{\mathbf{reg}}) \oplus (\boldsymbol{B} \oplus \boldsymbol{B} \oplus \cdots \oplus \boldsymbol{B})) \cap \boldsymbol{T}^c \tag{2}$$

where $\boldsymbol{B}$ occurs N_d times on the right hand side.

C. Intensity Normalization

Due to variations of the scanner and acquisition environment over time, the image intensities of a pair of repeat scans of a patient may not be directly comparable. Scaling image intensities on each scan to give the same mean over tissue which has not changed between the scans, to a first approximation, eliminates this variability.

We assume that tissue deeply interior to the brain (i.e., distant from the external boundary and any new internal boundaries associated with the appearance of new spaces or lesions) is largely unchanged. This is a reasonable approximation because the small changes we wish to measure are likely to represent only a small proportion of this region. In addition, structural readjustment should result in some degree

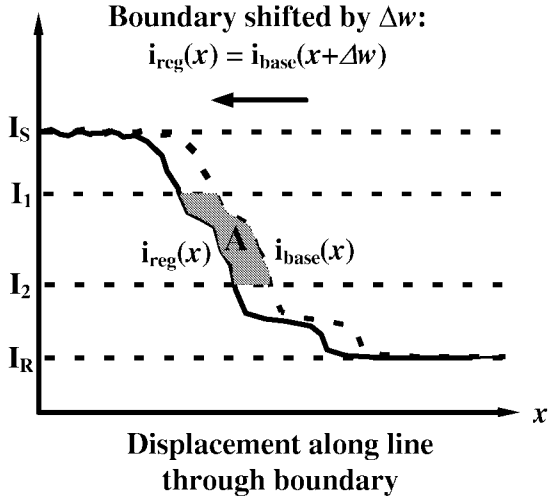

Fig. 2. A one-dimensional representation of a boundary shift between a baseline scan, $i_{\mathrm{base}}(x)$, and a registered repeat scan, $i_{\mathrm{reg}}(x)$. An estimate of the shift, Δw, may be obtained as the area $\boldsymbol{A}$ divided by $\boldsymbol{I_1 - I_2}$ (the intensity window).

of "substitution" of lost tissue, further limiting change over the interior of the brain. We therefore normalize the intensities on each scan by dividing by the mean intensity of the interior region ($\boldsymbol{T}$) of the brain, yielding unit mean over this region.

D. Boundary Shift Integral (BSI)

A change in volume of any object must be associated with an exactly equivalent shift in the boundaries of that object. We may therefore measure the change in volume of a cerebral structure by obtaining the total volume through which its boundaries shift.

As discussed previously, we assume that change near cerebral boundaries can be modeled as a simple shift of tissue, resulting in an exactly equivalent shift of the lowpass filtered signal which may be reconstructed from the MR samples. Hence, if $i_{\mathrm{base}}(x)$ is the lowpass filtered point MR response along a line on the baseline scan and $i_{\mathrm{reg}}(x)$ is the same response from a registered repeat scan on which there has been a boundary shift of Δw, then the responses must be related by

$$i_{\mathrm{reg}}(x) = i_{\mathrm{base}}(x + \Delta w) \tag{3}$$

in the region of the boundary.

If we assume there is a monotonic intensity change across the boundary, then $i_{\mathrm{base}}(x)$ and $i_{\mathrm{reg}}(x)$ will take the form shown in Fig. 2. We can, therefore, define inverse functions $x_{\mathrm{base}}(i)$ and $x_{\mathrm{reg}}(i)$, related by

$$x_{\mathrm{base}}(i) = x_{\mathrm{reg}}(i) + \Delta w. \tag{4}$$

A simple estimate of w may be obtained as $x_{\mathrm{base}}(I) - x_{\mathrm{reg}}(I)$, where I may be any value such that $I_R < I < I_S, I_S$ being the intensity within the bulk of the structure and I_R the intensity at the other side of the boundary. A more robust estimate may be obtained by averaging the estimates of Δw obtained over a range of I, such that

$$\Delta w = \frac{1}{I_1 - I_2} \int_{I_2}^{I_1} (x_{\mathrm{base}}(i) - x_{\mathrm{reg}}(i))\, di \quad \text{where } I_R \le I_2 < I_1 \le I_S. \tag{5}$$

This may alternatively be expressed as an integral with respect to x

$$\Delta w = \frac{1}{I_1 - I_2} \int_{\mathrm{boundary}} (\mathrm{clip}(I_{\mathrm{base}}(x), I_1, I_2) - \mathrm{clip}(i_{\mathrm{reg}}(x), I_1, I_2))\, dx \tag{6}$$

where

$$I_R \le I_2 < I_1 \le I_S$$

$$\mathrm{clip}\ (a, I_1, I_2) = \begin{cases} I_2 & a < I_2 \\ a & I_2 \le a \le I_1 \\ I_1 & a > I_1 \end{cases}. \tag{7}$$

Equations (5) and (6) may be confirmed to be equivalent by considering that both integrals evaluate the area labeled A in Fig. 2. The precise limits for the integration of (6) are $x_{\mathrm{reg}}(I_1)$ to $x_{\mathrm{base}}(I_2)$, however, outside these limits the integrand evaluates to zero, and hence, for simplicity, we have extended the limits to cover the whole boundary.

If we now extend this analysis to three-dimensions, we may determine the total volume displaced over the boundary of a structure as Δv, where

$$\Delta v = \frac{1}{I_1 - I_2} \iiint_{\mathrm{boundary}} (\mathrm{clip}\ (i_{\mathrm{base}}(x,y,z), I_1, I_2,) - \mathrm{clip}\ (i_{\mathrm{reg}}(x,y,z), I_1, I_2))\, dx\, dy\, dz \tag{8}$$

This integral may be determined numerically by evaluating the integrand at small sampling intervals, requiring the reconstruction of $i_{\mathrm{base}}(x,y,z)$ and $i_{\mathrm{reg}}(x,y,z)$ at these intervals. However, for simplicity, we choose the sampling intervals for the evaluation of the integral to be the same as on the original scans. Hence we approximate Δv by the *boundary shift integral* (BSI) which we define as

$$\mathrm{BSI} = \frac{K}{I_1 - I_2} \sum_{x,y,z \in \boldsymbol{E}} (\mathrm{clip}\ (I_{\mathrm{base}}(x,y,z), I_1, I_2) - \mathrm{clip}\ (I_{\mathrm{reg}}(x,y,z), I_1, I_2)) \tag{9}$$

where K is the product of the sampling intervals in each dimension (i.e., the voxel volume), $\boldsymbol{E}$ is the set of voxels in the boundary region [see (2)], and $I_{\mathrm{base}}(x,y,z)$ and $I_{\mathrm{reg}}(x,y,z)$ are the normalized voxel intensities on the registered scans. We refer to the range of the integral, $[I_2, I_1]$, as the intensity window, which we define in terms of its center $I_c = I_1/2 + I_2/2$, and width $I_w = I_1 - I_2$.

Note that the approximation between the BSI and v can be reduced to any desired level by subsampling the scans prior to evaluation. Hence, assuming consistent noiseless scan acquisition, the BSI may be used to measure volume change to arbitrarily high levels of accuracy—the acquisition voxel size places a limit only in that it determines the degree to which the desired boundary can be isolated from other boundaries.

E. Parameter Selection and Gain Estimation

Evaluation of the BSI over any structure requires the appropriate selection of an intensity window, (i.e., I_c and I_w), and sizes for the morphological operators (i.e., N_e and N_d). The intensity window should be selected such that it falls entirely within all of the intensity transitions associated with the boundaries of a structure—for typical structures within the brain this is complicated by adjacent structures having several different intensities and the structure itself being made up of tissues with differing intensities. Similarly, the morphological operator sizes should ideally be selected such that the boundary region includes the whole of the structure's boundary. However, maximizing the signal-to-noise ratio of the BSI, imposes counteracting constraints. The intensity window should be made as wide as possible, so as to maximize the number of contributing boundary voxels (i.e., signal); whereas the morphological operators should be made as small as possible (while still covering the entire boundary), to avoid extending the boundary region across more than one boundary and to minimize the number of contributing nonboundary voxels (i.e., noise).

The optimum set of parameters is primarily dependent upon the scan acquisition protocol, and the arrangement and intensity of adjacent tissue types with respect to the structure—none of which should vary substantially from patient to patient. We may, therefore, determine an optimum set for a given scan type and structure based upon a single subject.

This is performed by comparing simulated and measured volumes of loss over a range of parameter values. We simulate different volumes of loss in a given structure on a single scan, by spatially scaling the scan about the central point of the structure by equal amounts in each dimension. This yields a series of new scans, in each of which the volume of the structure has been artificially increased or decreased by a percentage that is known exactly. The BSI may then be evaluated between each of the resampled scans and the original, and plotted against the known change in volume (i.e., the corresponding percentage of the structure's volume as obtained by segmentation). Typically, these plots are very linear over a wide range of parameter values, however, the gradient of a linear fit to the points, which we refer to as the gain of the BSI, in general is less than the ideal of unity. We suggest that this is due to difficulties in determining an intensity window which is spanned by all the intensity transitions at the structure's boundaries, this leads to a failure to fully account for some boundary shifts. We select the optimum set of parameters as that which maximizes the gain of the BSI, although compromises must be made to obtain a sufficiently wide window (I_w) to ensure the measure is robust to noise.

IV. Quality Control

Patient motion during the scan results in phase errors in the MR signal which are observed on the scans as motion artifact. The level of artifact may vary widely between scans, being dependent upon the stillness of the patient. Where there is significant artifact the quality of image matching will be reduced and the BSI will represent a less reliable measure of volume change. We assess the level of motion artifact in a scan according to the figure m_o (see below) and discard scan pairs for which the mean m_o is greater than a threshold figure.

A. Measurement of Motion Artifact

One consequence of the motion-related phase errors is increased noise in voxels displaced from the head in the phase-encoding direction. We base our measure of motion artifact, m_o, on the level of this noise.

We define $\boldsymbol{S}_o$ as the set of all voxels between the head and the edge of the scan, along lines in the phase-encoding directions. We determine $\boldsymbol{S}_o$ automatically in five stages: 1) the scan is normalized by dividing each voxel intensity by the mean intensity over the brain (the brain having been previously identified for registration), 2) $\boldsymbol{S}_o$ is initialized to the null set, 3) every coronal slice is scanned left-to-right and right-to-left, and every voxel between the start of the row and the first voxel with intensity above 0.15 is added to $\boldsymbol{S}_o$ (where no voxel above this threshold is found $\boldsymbol{S}_o$ is unchanged), 4) $\boldsymbol{S}_o$ is dilated three times by the operator $\boldsymbol{B}$, and 5) $\boldsymbol{S}_o$ is eroded four times by the operator $\boldsymbol{B}$. As previously, the operator $\boldsymbol{B}$ consists of the origin and its six neighbors in three dimensions. The level of motion artifact, m_o, is calculated as the mean voxel intensity over the set $\boldsymbol{S}_o$.

In addition to motion, one would expect m_o to be directly influenced by other sources of noise; thermal noise in particular. To assess the degree to which m_o is dependent upon motion artifact, we ranked 20 scans (acquired as described in V) according to a visual assessment of the severity of motion related "ringing" artifact within brain. We compared our rankings with the m_o figure obtained for each scan and found a rank correlation coefficient of 0.76; suggesting that m_o is predominantly dependent upon the level of motion artifact.

V. Experiments

Baseline and repeat T1-weighted 3D MR scans were acquired from 14 normal control subjects and seven AD patients using a 1.5-T GE Signa unit with a spoiled gradient echo technique ($256 \times 128 \times 128$ matrix; $24 \times 24 \times 19.2$-cm field of vision (FOV); TR/TE/NEX/FLIP 35/5/1/35). Several subjects had further repeat scans, yielding a total of 22 control scan pairs and 15 AD scan pairs, all with scan intervals of one year $\pm$ three months).

The parameter selection procedure was performed for both whole brain BSI and ventricular system BSI. The procedures utilized a single control scan and 32 levels of simulated volume change (-8% to $+8\%$ in steps of 0.5%). The selected parameter sets were used in the following stages.

All baseline-repeat scan pairs were registered as previously described [2]. We calculated the motion artifact figure, m_o, and the residual registration error over the brain, r_{err}, where

$$r_{\text{err}} = \frac{\Sigma_{\text{brain}} |I_1(x,y,z) - I_2(x,y,z)|}{N_{\text{vox}}} \tag{10}$$

and N_{vox} is the number of voxels corresponding to brain. The brain BSI and ventricular BSI were calculated between

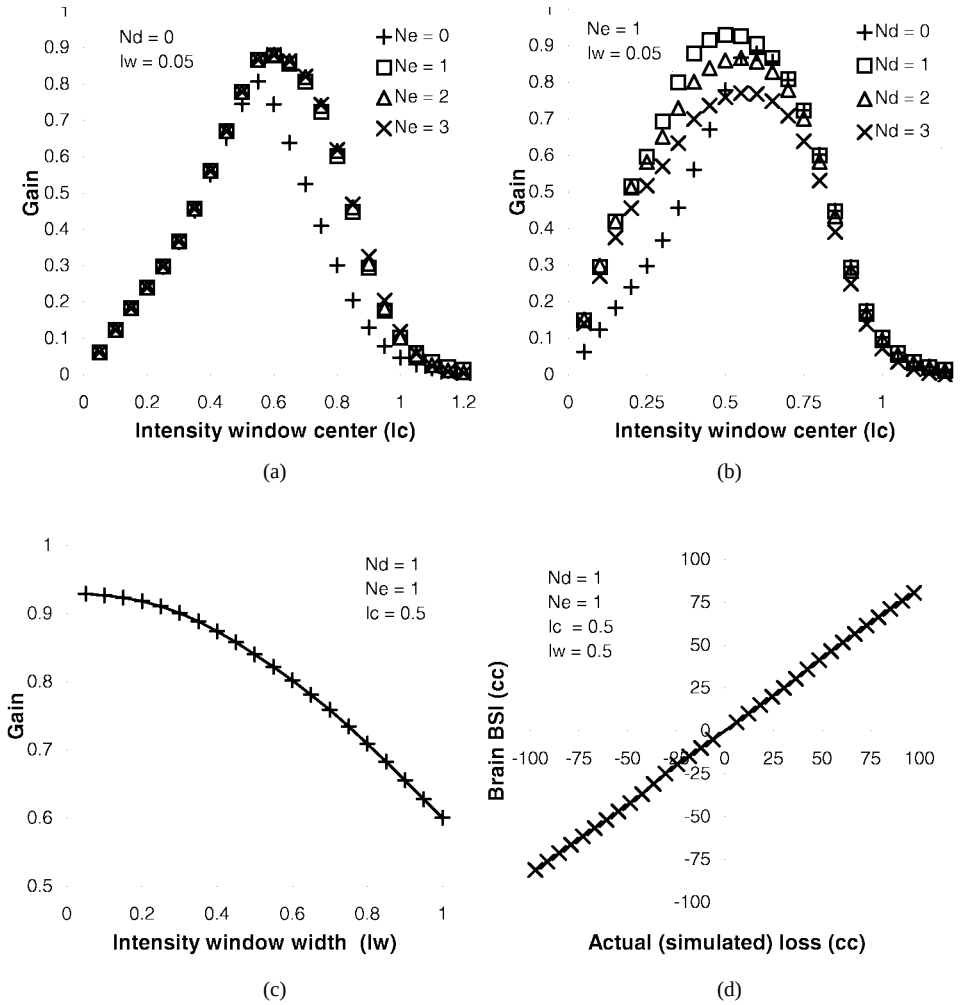

Fig. 3. (a)–(c) Dependence of the gain of the brain BSI (determined by the simulation procedure) on the measurement parameters: N_e, size of erosion operator; N_d, size of dilation operator; I_c, center of intensity window; I_w, width of intensity window. (d) The relation between the brain BSI and simulated volume loss for the selected parameter set $N_e = 1, N_d = 1, I_c = 0.5$ and $I_w = 0.5$.

those scan pairs for which the mean m_o was less than 0.047 (arbitrarily selected to reject only the most severe cases). A Sparc20 workstation (Sun Microsystems Inc., Palo Alto, CA) was used for computation.

VI. Results and Discussion

Fig. 3 shows the effect of the measurement parameters (N_d, N_e, I_c, and I_w) on the gain of the brain BSI. Initially, we used a narrow intensity window and no dilations ($I_w = 0.05, N_d = 0$), and varied the size of the erosion operator (N_e) and the window center (I_c). With $N_e = 0$ the gain was found to peak at 0.81 with $I_c = 0.55$, for $N_e = 1$ the gain peaked at 0.88 with $I_c = 0.6$, but further increases in N_e had no effect upon gain [Fig. 3(a)]. This suggests that with no erosion the inner border of the brain boundary region does not extend sufficiently into the brain. Sufficient extension is obtained by use of an erosion operator with $N_e = 1$, but further increases in N_e have no benefit. Note that this inward extension of the boundary region also resulted in an increased I_c at the peak—a consequence of a greater proportion of high-intensity changes being included in the boundary region. We selected $N_e = 1$ as optimum.

Using a narrow intensity window $(I_w = 0.05)$ and fixing N_e at one, we varied the size of the dilation operator (N_d) and the window center (I_c). With $N_d = 0$ the gain was found to peak at 0.88 with $I_c = 0.6$, for $N_d = 1$ the gain peaked at 0.93 with $I_c = 0.5$, but further increases in N_d led to a reduction in gain [Fig. 3(b)]. This suggests that with no dilation, the boundary region does next extend sufficiently away from brain, and that sufficient coverage requires a dilation operator with size $N_d = 1$, however, use of a larger operator distorts the measure by including boundaries not associated with brain. The increased outward extension of the boundary region also resulted in a decrease in I_c at the peak—this is associated with a greater proportion of low intensity changes being included in the boundary region. We selected $N_d = 1$ and $I_c = 0.5$ as optimum.

Fixing $N_e = 1, N_d = 1$ and $I_c = 0.5$, we varied the width of the intensity window, I_w, from 0.05 to 1.0 and found that gain steadily reduced with increasing I_w [Fig. 3(c)]. This may have been predicted as increasing the intensity window width must result in a smaller proportion of the intensity transitions at the boundaries of the brain fully spanning the intensity window, leading to a reduction in gain. However, obtaining a measure

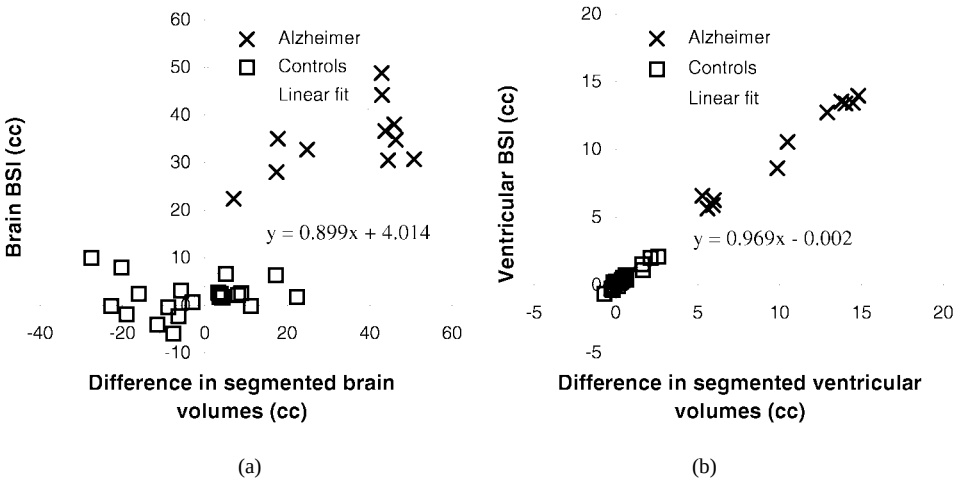

(a) (b)

Fig. 4. (a) The brain BSI plotted against difference in segmented brain volume (based on the same region definitions used to generate the boundary region) for 11 AD and 21 control scan pairs. (b) The corresponding comparison of the ventricular BSI with difference in segmented ventricular volume. The linear fits were based on minimizing error in the segmentation measure (x-axis).

robust to noise requires a wide window, such that the range of intensities over which the boundary shift is averaged is large (Fig. 2). We arbitrarily chose to trade 10% of the peak gain for an increased window size and, hence, adopted $I_w = 0.5$, giving a gain of 0.84.

Fig. 3(d) shows the brain BSI for different levels of volume change, evaluated using the selected parameters ($N_e = 1, N_d = 1, I_c = 0.5$ and $I_w = 0.5$). The relation closely approximates linearity (product-moment $r = 1.000$).

The results from parameter selection (Fig. 3) indicate that the gain is not critically dependent upon the exact selection of measurement parameters—similar levels of gain are maintained over a relatively wide range of parameters. This supports the use of parameters determined for a given structure from a single subject, in all subjects scanned using the same protocol.

Applying the same parameter selection procedure to the ventricular BSI we observed identical trends, resulting in the selection of $N_e = 1, N_d = 1, I_c = 0.6$, and $I_w = 0.5$, yielding a correlation of $r = 0.999$ and predicted gain of 1.10. The optimum intensity window is higher than that obtained for brain, as there is a greater proportion of white matter around the ventricular surface as compared to the brain surface as a whole (white matter appearing brighter than gray matter in T1 MR scans). Note, also, that the predicted gain is greater than one, whereas we have argued that the BSI should generally yield a gain of less than one. We suggest that the prediction is actually an overestimate—a result of an underestimate in the segmented ventricular volume from which the volume of simulated atrophy is determined (by taking percentages). Our ventricular segmentation method is highly sensitive to the threshold selected to detect the boundary. We utilized a threshold of 0.5 of the mean brain intensity, whereas the selection of $I_c = 0.6$ suggests that this is not the center of the intensity transition and that, hence, we are underestimating our actual volumes of simulated atrophy. This does not undermine the parameter selection method, as the optimum parameters will still correspond to the peak gain.

In the 22 control scan pairs, we compared the motion artifact measure, m_o, to the residual registration mismatch and found a significant correlation (product-moment $r = 0.532, p = 0.01$), demonstrating that motion artifact is a major source of noise that we must control. We chose to reject only those scan pairs with the highest levels of motion artifact; we adopted a threshold m_o of 0.047 leading to the rejection of four AD and one control scan pair. In general we have found a larger prevalence of motion artifact in scans of AD patients. This reinforces the need to control for the artifact—to inhibit a possible causal relation between symptoms (i.e., forgetting to remain still) and the BSI. However, scan rejection in this manner is undesirable for routine clinical use, and we are currently investigating the use of head restraints and other devices to reduce patient motion.

For the remaining 21 control and 11 AD scan pairs, the mean scan intervals were 384 and 388 days, respectively. Fig. 4(a) shows the brain BSI plotted against the difference in absolute segmented volumes, the latter being based upon the same region definitions used to generate the boundary region. The BSI yielded mean brain volume loss of 1.8 cc (controls) and 34.7 cc (AD); the control group was tightly bunched (SD = 3.8 cc) and there was wide group separation, the group means differing by 8.7 control group SD's. The segmentation measure yielded similar group means, but wide spread in the control group (SD = 13.4 cc) and group overlap, the group means differing by 2.8 control group SD's (see also Table I). This demonstrates that the BSI provides a measure, substantially more accurate than the segmentation upon which it is based. Fitting a linear regression line (to minimize error in the segmentation measure), we obtained a gradient of 0.90; this compares to the gain of 0.84 predicted by the simulation procedure.

Fig. 4(b) similarly shows the ventricular BSI plotted against the difference in absolute segmented volumes. In contrast to their application to brain, there is very tight correlation between the two measures ($r = 0.997$). The mean volume loss obtained by the BSI as 0.4 cc in the control group and 10.1 cc in the AD group; these compare to 0.5 cc and 10.3 cc

TABLE I
MEAN SD SCAN INTERVALS AND MEASURES OF VOLUME LOSS FOR THE 21 CONTROL AND 11 AD REPEAT SCAN PAIRS. THE MEAN SD VOLUME LOSS IS SHOWN FOR BOTH TOTAL BRAIN AND VENTRICLES, AND IN EACH CASE AS MEASURED BY BOTH THE BOUNDARY SHIFT INTEGRAL (BSI) AND THE SEGMENTATION MEASURE

	Scan Interval/days	Total Brain/cc		Ventricles/cc	
		BSI	Segmentation	BSI	Segmentation
Controls	348(70)	1.8(3.8)	−2.9(13.4)	0.4(0.7)	0.5(0.8)
AD	388(48)	34.7(7.3)	34.9(15.1)	10.1(3.5)	10.3(3.9)

obtained by segmentation (see Table I). The ventricles are a simple structure with very sharp defining boundaries and may be accurately segmented by semiautomated methods. These results, therefore, further confirm that the BSI provides a linear measure of volume change. Again fitting a linear regression line, we obtained a line of gradient 0.97, which compares to the gain of 1.10 predicted by the simulation procedure.

Note that segmentation errors merely influence the sensitivity of the BSI (by distorting the boundary region) and do not introduce large biases, as occurs when comparing absolute volumes. This is likely to be the predominant reason for the improved accuracy of the brain BSI as compared to segmentation.

The brain BSI was found to slightly underestimate volume change (gain less than unity). For complex structures with several defining boundaries, it is unlikely that a single, sufficiently-wide, intensity window will be spanned by all the possible intensity transitions at its boundaries; hence, loss tends to be underestimated. The parameter selection procedure aims to assess and minimize the degree of underestimate, by determining an intensity window which is spanned by most boundaries. Note also that where a structure is bounded by regions, both of higher and lower intensity, two intensity windows may be needed to account for the two possible directions of change.

A prerequisite for use of the BSI is that the boundaries between a structure and adjacent tissue involve an intensity transition from one MR signal intensity to another. Indeed, this is the basis upon which cerebral structures are discerned on magnetic resonance imaging (MRI). Where the majority of a structure's boundaries do not involve such a transition, the BSI is likely to be a considerable underestimate of the volume of change; however, in such cases, measurement of volume change by any method is likely to be problematic. Where a lesser proportion of the boundary fails to involve an intensity transition (e.g., structures such as cortical gyri, which do not have definitive borders on all sides), the BSI may, in principle, still yield a good estimate, whereas comparison of segmented volumes is likely to be unreliable.

VII. CONCLUSIONS

We propose the BSI as a measure of volume change between repeat MR scans. We have found the BSI to be a linear and accurate measure of change—levels of accuracy far higher than the underlying segmentation may be obtained. The method can be utilized to yield both global and regional measures of change. The BSI may be of use in the diagnosis of neurodegenerative diseases, assessment of disease progression, and evaluation of potential treatments.

ACKNOWLEDGMENT

The authors would like to thank Dr. M. Rossor of the National Hospital for Neurology and Neurosurgery, London, U.K., for his support and advice and Dr. P. Tofts of the Institute of Neurology, London, U.K.

REFERENCES

[1] N. C. Fox, P. A. Freeborough, and M. N. Rossor, "Visualization and quantification of atrophy in Alzheimer's disease," *Lancet*, vol. 348, pp. 94–97, 1996.
[2] P. A. Freeborough, R. P. Woods, and N. C. Fox, "Accurate registration of serial 3D MR brain images and its application to visualizing in change in neurodegenerative disorders," *J. Comput. Assist. Tomogr.*, vol. 20, pp. 1012–1022, 1996.
[3] S. J. Nelson, B. S. Nalbandian, E. Proctor, and D. B. Vigneron, "Registration of images from sequential MR studies of the brain," *J. Magn. Reson. Imag.*, vol. 4, pp. 877–883, 1994.
[4] J. V. Hajnal, N. Saeed, A. Oatridge, E. J. Williams, I. R. Young, and G. M. Bydder, "Detection of subtle brain changes using subvoxel registration and subtraction of serial MR images," *J. Comput. Assist. Tomogr.*, vol. 19, pp. 677–691, 1995.
[5] J. V. Hajnal, N. Saeed, E. J. Soar, A. Oatridge, I. R. Young, and G. M. Bydder, "A registration and interpolation procedure for subvoxel matching of serially acquired MR images," *J. Comput. Assist. Tomogr.*, vol. 19, pp. 289–296, 1995.
[6] P. A. Freeborough and N. C. Fox, "Scaling compensation in the registration of serial 3D MRI of the brain," in *Proc. ISMRM*, 1996, vol. 3, p. 1654.
[7] K. H. Hohne and W. A. Hanson, "Interactive segmentation of MRI and CT volumes using morphological operations," *J. Comput. Assist. Tomogr.*, vol. 16, pp. 285–294, 1992.
[8] P. A. Freeborough, N. C. Fox, and R. I. Kitney, "Accurate segmentation of 3D brain scans: Interactive software and algorithms," *Comput. Meth., Programs Biomed.*, vol. 53, pp. 15–25.